Local structural displacements across the structural phase transition in $IrTe_2$: Order-disorder of dimers and role of Ir-Te correlations

B. Joseph,[1] M. Bendele,[1] L. Simonelli,[2] L. Maugeri,[1] S. Pyon,[3] K. Kudo,[3] M. Nohara,[3] T. Mizokawa,[4] and N. L. Saini[1]

[1]*Dipartimento di Fisica, Universitá di Roma "La Sapienza" - P. le Aldo Moro 2, 00185 Roma, Italy*

[2]*European Synchrotron Radiation Facility, BP220, F-38043 Grenoble Cedex, France*

[3]*Department of Physics, Okayama University, Kita-ku, Okayama 700-8530, Japan*

[4]*Department of Complexity Science and Engineering, University of Tokyo, 5-1-5 Kashiwanoha, Chiba 277-8561, Japan*

(Received 30 October 2013; published 31 December 2013)

We have studied local structure of $IrTe_2$ by Ir L_3-edge extended x-ray absorption fine structure (EXAFS) measurements as a function of temperature to investigate origin of the observed structural phase transition at $T_s \sim 270$ K. The EXAFS results show an appearance of longer Ir-Te bond length ($\Delta R \sim 0.05$ Å) at $T < T_s$. We have found Ir-Ir dimerization, characterized by distinct Ir-Ir bond lengths ($\Delta R \sim 0.13$ Å), existing both above and below T_s. The results suggest that the phase transition in $IrTe_2$ should be an order-disorder-like transition of Ir-Ir dimers assisted by Ir-Te bond correlations, thus indicating important role of the interaction between the Ir $5d$ and Te $5p$ orbitals in this transition.

DOI: 10.1103/PhysRevB.88.224109 PACS number(s): 74.70.Xa, 74.81.−g, 61.05.cj, 74.62.Bf

Recently, the layered $5d$-transition-metal dichalcogenide $IrTe_2$ has been in the limelight after the observation of superconductivity in $Ir_{1-x}Pt_xTe_2$ with T_c of about 3 K.[1] This observation was followed by several studies revealing superconductivity due to intercalation addition and/or substitution by different metals in the parent $IrTe_2$.[2–4] It has been argued that the superconductivity might be induced by Ir vacancies or excess Te in the sample.[5] On the other hand, the parent $IrTe_2$ exhibits a first-order structural phase transition[5–8] at $T_s \sim 270$ K from the trigonal (P-$3m1$) at $T > T_s$ to a lower-symmetry phase at $T < T_s$, accompanied by an anomalous electrical and magnetic transport.[1] Since the superconductivity is induced with concomitant suppression of structural phase transition, the origin of this transition in $IrTe_2$ remains one of the intriguing physical problems.[1–5,8–11]

The structural phase transition in $IrTe_2$ has been argued to be similar to the one observed in the spinel-type $CuIr_2S_4$,[12] showing Ir-Ir dimerization. A recent angle-resolved photoemission spectroscopy (ARPES) study[13] has shown that, in the trigonal phase ($T > T_s$), the Fermi surface consists of a flower-shaped outer part and six connected bead-like inner parts, consistent with the band-structure calculations. In the low-temperature phase ($T < T_s$) the flower shape of the outer Fermi surface does not change appreciably; however, the topology of the inner Fermi surface reveals straight portions, suggesting possible Fermi-surface nesting.[13] The perfect or partial nesting of Fermi surface can induce a charge density wave (CDW) and hence a superstructure, as observed by electron diffraction below the structural phase transition.[2] However, the gap opening expected for a CDW was not observed,[14] suggesting that the structural transition in $IrTe_2$ may not be of conventional CDW type but could involve Te $5p$ orbitals.[5] Therefore, the two main issues to be addressed are (i) is the structural phase transition driven by some kind of dimerization? and (ii) what is the role of Ir and Te bonding (i.e., Ir $5d$ and Te $5p$ hybridization) in the phase transition? To affront these questions we have studied the local structure of $IrTe_2$ by Ir L_3-edge extended x-ray absorption fine structure (EXAFS) measurements as a function of temperature, providing direct information on the first-order atomic correlation functions across the structural phase transition. We have found clear evidence of dimerization in $IrTe_2$ characterized by two different Ir-Ir distances separated by ∼0.13 Å. The dimerization survives even above the phase transition temperature; however, two distinct Ir-Te distances ($\Delta R \sim 0.05$ Å) at low temperature merge in a single distance above the transition, highlighting the importance of the (Ir $5d$)-(Te $5p$) hybridization.

The $IrTe_2$ samples were prepared by solid-state reaction starting from stoichiometric amounts of Ir and Te. Details on the sample preparation and characterization are given elsewhere.[1] Temperature-dependent Ir L_3-edge ($E =$ 11 215 eV) x-ray absorption measurements, in the range 20 to 300 K, on powder samples of $IrTe_2$, were performed in transmission mode at the beamline BM26A[15] of the European Synchrotron Radiation Facility (ESRF), Grenoble (France). The synchrotron radiation emitted by a bending magnet source was monochromatized using a double crystal Si(111) monochromator. Several scans were collected at a given temperature to ensure the spectral reproducibility. The EXAFS oscillations were extracted using the standard procedure based on the spline fit to the pre-edge subtracted absorption spectrum.[16]

Figure 1 shows EXAFS oscillations (multiplied by k^2), extracted from Ir L_3-edge x-ray absorption spectra, measured on $IrTe_2$ at several temperatures. The oscillations are clear up to high k range even at high temperature. Apart from the thermal damping, the EXAFS oscillations reveal some apparent changes across the structural phase transition temperature of about 270 K. For example, ∼13 Å^{-1} the double peak structure becomes single-peak like, different from an expected thermal damping. Similarly, around 14 Å^{-1} the asymmetric shape of the peak becomes more symmetric above T_s. The differences can be further seen in the partial atomic distribution function around the photoabsorbing atoms, given by the Fourier transform (FT) of the EXAFS oscillations.

Figure 2 shows the FT magnitudes of the EXAFS oscillations. The FTs are performed in the k range of 3 to 17 Å^{-1} using a Gaussian window. The main peak in the FTs is due to six near-neighbor Te atoms at ∼2.6 Å. The next-nearest neighbors are the Ir atoms (at ∼3.8 Å) and their

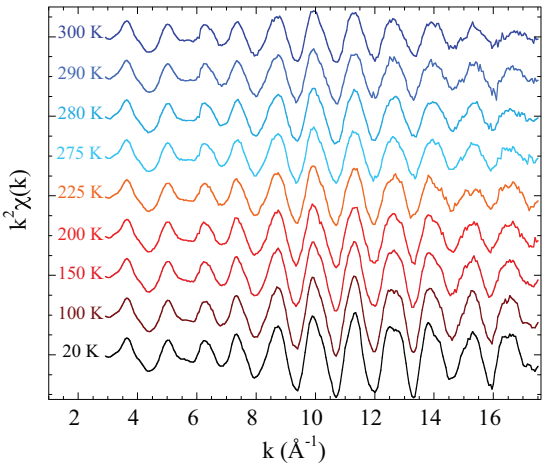

FIG. 1. (Color online) Ir L_3-edge EXAFS oscillations (weighted by k^2) at several temperatures. Apart from a temperature-dependent damping, some small changes can be seen across $T = 270$ K (see, for example, k around 14 Å^{-1}).

contributions appear around ∼3.5–4.5 Å. The weak signal of the latter indicates that the system is characterized by a large intrinsic disorder, consistent with polymeric networks.[9] The large intrinsic disorder is also apparent from highly damped FT intensity of higher shells.

The local structure parameters as a function of temperature are determined by standard EXAFS modeling based on the single-scattering approximation.[16] In the present case, we used a model with two Ir-Te and two Ir-Ir bond lengths, similar to the low-temperature-diffraction observations.[2,11,17] The EXCURVE 9.275 code (with calculated backscattering amplitudes and phase-shift functions) was used for the EXAFS model fits.[18] The radial distances R_i and the corresponding Debye–Waller factors σ_i^2 were allowed to vary in the least-squares fits. The coordination number for the near neighbors N_i were obtained by a constrained refinement with the total number of near neighbors being equal to known values from diffraction studies describing the long-range structure. For the present analysis,

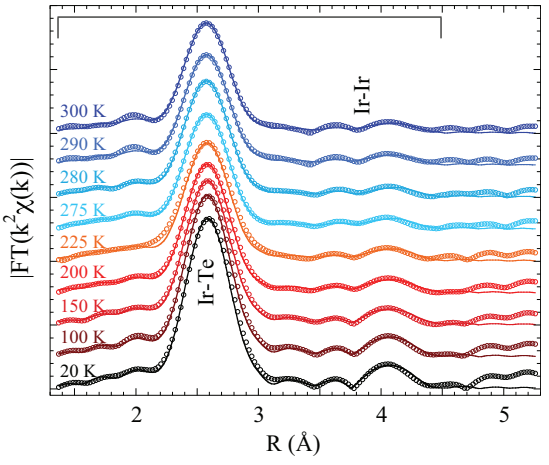

FIG. 2. (Color online) Fourier transform magnitudes of the EXAFS oscillations (weighted by k^2) at several temperatures (symbols) together with model fits (solid lines). The fit range in the R space is indicated by a bracket on the top.

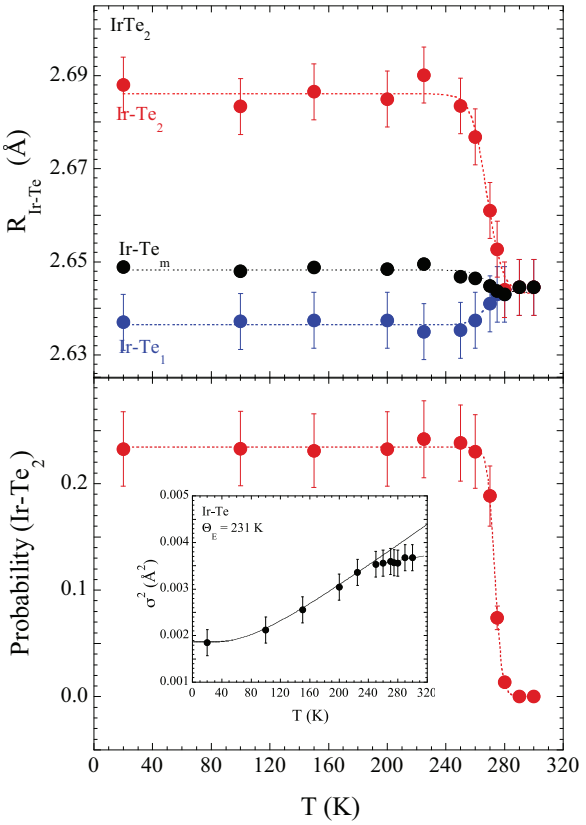

FIG. 3. (Color online) Temperature dependence of two Ir-Te distances (Ir-Te$_1$ and Ir-Te$_2$) as a function of temperature (upper panel). The mean bond length Ir-Te$_m$ is also included. The relative probability of the Ir-Te$_2$ bond length is shown in the lower panel. The dashed lines are to guide the eyes and show a clear transition at ∼270 K. The inset shows the temperature dependence of the Ir-Te bond length MSRD. The solid line in the inset is a Einstein model fit with the $\theta_E = 231 \pm 20$ K for $T < T_s$.

the number of independent data points, $N_{\text{ind}} \sim (2\Delta k \Delta R)/\pi$[16] were about 25 ($\Delta k = 13$ Å^{-1} and $\Delta R = 3$ Å), for a maximum of twelve parameters fits. The uncertainties in the local structure parameters were determined by creating correlation maps and analyzing five different scans. The model fits in real space using four shells are shown in Fig. 2 as solid lines.

Figure 3 shows the temperature dependence of local Ir-Te bond lengths (see, e.g., the upper panel of Fig. 3). There are two Ir-Te distances (∼2.69 Å and ∼2.64 Å) below the structural phase transition temperature $T_s \sim 270$ K, that appear to merge in a single distance (∼2.65 Å) above T_s. The relative probability of the longer distance, which is 20% to 30% of the total number of Ir-Te bonds below the transition temperature, drops down to zero while heating across the transition (see lower panel of Fig. 3). This observation is in fair agreement with diffraction studies that show almost one third of the (two out of six) Ir-Te bonds to be longer.[2,11,17] The longer Ir-Te distance appears consistent with the recent structural studies[11,17] where the deformation of the $IrTe_6$ octahedron is identified with about 2% variation of the Ir-Te distance across the structural phase transition.

The Debye–Waller factors measured by EXAFS describe mean-square relative displacements (MSRD) unlike the one

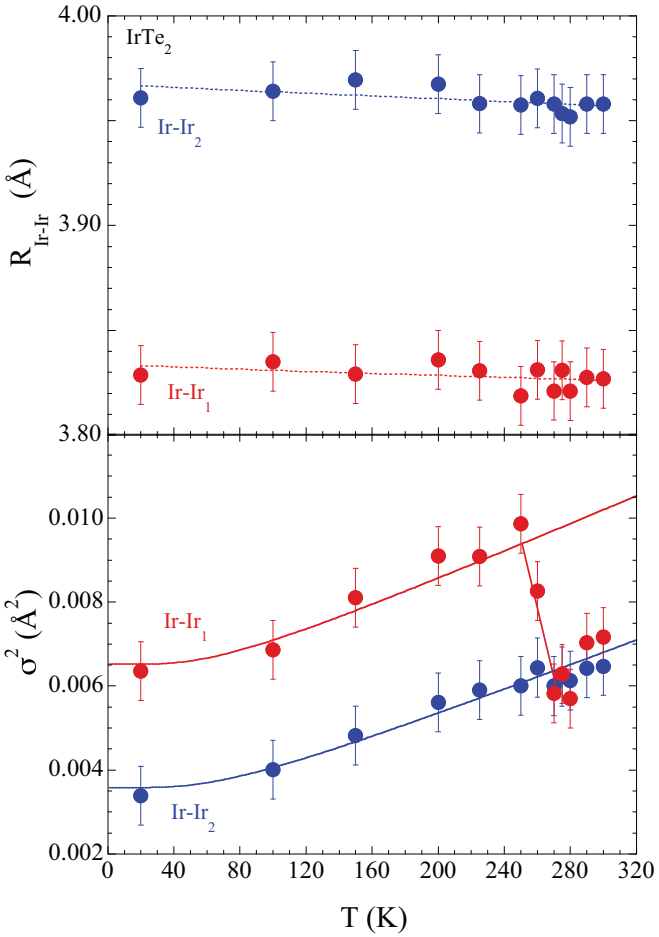

FIG. 4. (Color online) The Ir-Ir distances (Ir-Ir_1 and Ir-Ir_2) are shown as a function of temperature (upper panel). The MSRD for the two Ir-Ir bond lengths are shown in the lower panel. The solid lines show Einstein-model fits with $\theta_E = 200$ K. The MSRD of the Ir-Ir_1 bond length shows an anomalous drop around the structural phase transition.

measured in diffraction studies, providing information on mean-square displacements (MSDs). Therefore, MSRD provides information on the bond-length fluctuations and has been particularly useful to understand local atomic displacements across phase transitions (see, for example, Refs. 19–22). The measured MSRD is sum of temperature independent and temperature dependent parts [i.e., $\sigma_i^2 = \sigma_0^2 + \sigma^2(T)$]. In the present case, the MSRD of the two Ir-Te distances are similar, given by the Einstein model[23] with the $\theta_E = 231 \pm 20$ K. If one distance model is used, the MSRD of Ir-Te bond-length (Ir-Te_m) shows anomalous temperature dependence across the phase transition (see, e.g., inset of Fig. 3). Therefore, the Ir-Te bond-length correlations (shown by ΔR, Ir-Te_2 probability and the MSRD anomaly) are directly tied to the first-order structural phase transition in $IrTe_2$.

Figure 4 shows the temperature evolution of Ir-Ir bond lengths. Unlike Ir-Te, the two Ir-Ir bond-lengths remain almost temperature independent and the splitting persists even above T_s. The presence of two different Ir-Ir distances is consistent with the diffraction studies at low temperature;[1,6,8] however, unlike the diffraction studies, distinct Ir-Ir bond lengths at the local scale persist even above the transition temperature. Here, we should recall a recent systematic diffraction study by Cao *et al.*[8] showing the low-temperature symmetry of $IrTe_2$ being triclinic rather than the earlier proposed monoclinic.[7] In addition, the newly established low-temperature diffraction structure[8] shows that the probability of the short Ir-Ir bond length is about 1/5; that is, in excellent agreement with the present results revealing the probability for the shorter bonds (Ir-$Ir_1 \sim 3.83$ Å) to be ∼20%.

Interestingly, the MSRD of the shorter bond length shows an anomalous change around T_s (Fig. 4). Indeed, the MSRD of the two Ir-Ir bond lengths can be described by the correlated Einstein model[23] with a similar Einstein temperature ($\theta_E = 200 \pm 15$ K) up to the structural phase transition, albeit with different σ_0^2 (∼0.002 and ∼0.005, respectively). Close to T_s the MSRD of the shorter Ir-Ir bond length (Ir-Ir_1) shows an abrupt decrease down to the values similar to the one for the longer (Ir-Ir_2) bond. This abrupt change in the MSRD provides an indication of some electronic topological change associated with the transition. It is worth noting that the ARPES studies reveal a clear change in the Fermi-surface topology across the transition.[13] Nevertheless, the results reveal that there are local Ir-Ir dimers in $IrTe_2$, and they have a clear role in the structural phase transition, further supported by the unusual temperature dependence of the MSRD of the Ir-Ir_1 bond lengths.

Let us discuss the implication of the present findings in relation to the highly debated question on the origin of the structural phase transition in $IrTe_2$. In the beginning, the first-order structural phase transition was thought to be similar to that in spinel $CuIr_2S_4$, in which the structural transition occurs from cubic to tetragonal due to the orbitally induced Peierls state below T_s.[1,14] Actually, a superstructure was observed at low temperature and it was argued that the structural phase transition in $IrTe_2$ is of CDW type.[2] However, the absence of a CDW gap across the phase transition does not support the conventional density-wave-like Fermi-surface instability being responsible for the structural phase transition,[14] but the crystal-field effect should have a prominent role in splitting the Te p_{xy} and Te p_z energy levels and reduction of the kinetic energy of the electronic system.[5] Similarly, it was also suggested that the interlayer and intralayer hybridizations play important roles in the structural phase transition, rather than the instability of Ir t_{2g} orbitals. A weak interlayer orbital hybridization causes the phase transition while stronger hybridization suppresses it.[3] Furthermore, the first-order structural phase transition has been related with polymeric networks of covalent Te-Te bonds in the adjacent Te layers, going under a reversible depolymerization below the transition temperature.[9] These arguments are consistent with the studies on pyrite-type $IrTe_2$ as a function of pressure, underlining the importance of Te-Te bond polymerization in the structural phase transition.[24] On the basis of a detailed study of low-temperature structure and first-principles calculations, it has been shown that a local bonding instability associated with the Te 5p states is likely the origin of the structural phase transition in $IrTe_2$.[8] Yet, more pressure-effect studies on $IrTe_2$ are found to be analogous to those of spinel $CuIr_2S_4$,[10] again keeping the debate wide open on the roles of Te 5p versus Ir 5d orbitals to drive the structural phase transition. In this context, our findings provide important information on the origin of the phase transition. We find that

both Ir-Te and Ir-Ir bonds are active players in driving the structural phase transition in $IrTe_2$. Indeed, the experimental results suggest that Ir-Ir dimers are present across the structural phase transition while Ir-Te bond lengths split only below the transition temperature. Since the charge superstructure appears below the transition temperature,[2] it should be related to the Ir-Ir dimers which are getting ordered. Therefore, it appears that the structural transition should be of order-disorder-like transition of Ir-Ir dimers driven by the Fermi-surface nesting[14] or by local singlet formation, where the ordering of dimers is assisted by the interaction between the Ir $5d$ and Te $5p$ orbitals. This situation is somewhat similar to the metal-insulator transition in VO_2, where V-V dimer formation is assisted by the Jahn–Teller-like interaction between the V $3d$ and O $2p$ orbitals.[25]

In summary, the local structure investigation of the $IrTe_2$ system provides detailed insight into the nature of the first-order phase transition occurring in the system at ~270 K. The results reveal that the Ir-Te distances are split in two at low temperature and merge in a single distance above the transition. We also find clear existence of distinct Ir-Ir bond lengths, indicating Ir-Ir dimerization. The local dimers survive even above the phase transition temperature. However, at the phase transition, the static disorder of Ir-Ir anomalously drops down. Therefore, the present results provide clear evidence of the importance of both Ir $5d$ and Te $5p$ orbitals in the structural phase transition. Combining the present results with earlier experiments,[5,14] it appears that, in the first-order phase transition of the $IrTe_2$ system, the Ir-Ir dimers undergo an order-disorder-like transition driven by the interaction between the Ir $5d$ and Te $5p$ orbitals.

We thank Sergey Nikitenko of BM26A, ESRF, Grenoble for support in the EXAFS data collection. The work is a part of the bilateral agreement between the Sapienza University of Rome and the University of Tokyo. One of us (M.B.) acknowledges the financial support of the Swiss National Science Foundation, Project No. PBZHP2_143495.

[1] S. Pyon, K. Kudo, and M. Nohara, J. Phys. Soc. Jpn. **81**, 053701 (2012).
[2] J. J. Yang, Y. J. Choi, Y. S. Oh, A. Hogan, Y. Horibe, K. Kim, B. I. Min, and S.W. Cheong, Phys. Rev. Lett. **108**, 116402 (2012).
[3] M. Kamitani, M. S. Bahramy, R. Arita, S. Seki, T. Arima, Y. Tokura, and S. Ishiwata, Phys. Rev. B **87**, 180501 (2013).
[4] K. Kudo, M. Kobayashi, S. Pyon, and M. Nohara, J. Phys. Soc. Jpn. **82**, 085001 (2013).
[5] A. F. Fang, G. Xu, T. Dong, P. Zheng, and N. L. Wang, Sci. Rep. **3**, 1153 (2013).
[6] S. Jobic, P. Deniard, R. Brec, J. Rouxel, A. Jouanneaux, and A. N. Fitch, Z. Anorg. Allg. Chem. **598**, 199 (1991).
[7] N. Matsumoto, K. Taniguchi, R. Endoh, H. Takano, and S. Nagata, J. Low Temp. Phys. **117**, 1129 (1999).
[8] H. Cao, B. C. Chakoumakos, X. Chen, J. Yan, M. A. McGuire, H. Yang, R. Custelcean, H. Zhou, D. J. Singh, and D. Mandrus, Phys. Rev. B **88**, 115122 (2013).
[9] Yoon Seok Oh, J. J. Yang, Y. Horibe, and S.-W. Cheong, Phys. Rev. Lett. **110**, 127209 (2013).
[10] A. Kiswandhi, J. S. Brooks, H. B. Cao, J. Q. Yan, D. Mandrus, Z. Jiang, and H. D. Zhou, Phys. Rev. B **87**, 121107(R) (2013).
[11] G. L. Pascut, K. Haule, M. J. Gutmann *et al.*, arXiv:1309.3548.
[12] P. G. Radaelli, Y. Horibe, M. J. Gutmann *et al.*, Nature (London) **416**, 155 (2002).
[13] D. Ootsuki, S. Pyon, K. Kudo *et al.*, J. Phys. Soc. Jpn. **82**, 093704 (2013).
[14] D. Ootsuki, Y. Wakisaka, S. Pyon *et al.*, Phys. Rev. B **86**, 014519 (2012).
[15] S. Nikitenko, A. M. Beale, A. M. J. van der Eerden *et al.*, J. Synchrotron Radiat. **15**, 632 (2008).
[16] *X-ray Absorption: Principles, Applications, Techniques of EXAFS, SEXAFS, XANES*, edited by R. Prins and D. C. Koningsberger (Wiley, New York, 1988).
[17] T. Toriyama, M. Kobori, and T. Konishi *et al.* (unpublished).
[18] S. J. Gurman, J. Synchrotron Radiat. **2**, 56 (1995).
[19] N. L. Saini, A. Lanzara, A. Bianconi, H. Oyanagi, H. Yamaguchi, K. Oka, and T. Ito, Phys. C **268**, 121 (1996).
[20] M. C. Sánchez, G. Subías, J. Garcïa, and J. Blasco, Phys. Rev. Lett. **90**, 045503 (2003).
[21] L. Downward, F. Bridges, S. Bushart, J. J. Neumeier, N. Dilley, and L. Zhou, Phys. Rev. Lett. **95**, 106401 (2005).
[22] F. Bridges, L. Downward, J. J. Neumeier, and T. A. Tyson, Phys. Rev. B **81**, 184401 (2010).
[23] J. J. Rehr and R. C. Albers, Rev. Mod. Phys. **72**, 621 (2000).
[24] J. M. Leger, A. S. Pereira, J. Haines, S. Jobic, and R. Brec, J. Phys. Chem. Solids **61**, 27 (2000).
[25] M. W. Haverkort, Z. Hu, A. Tanaka *et al.*, Phys. Rev. Lett. **95**, 196404 (2005).